Int. J. Heat Mass Transfer. Vol. 18, pp. 1409–1413. Pergamon Press 1975. Printed in Great Britain

RADIATION CHARACTERISTICS OF HONEYCOMB SOLAR COLLECTORS

C. L. TIEN and W. W. YUEN
Department of Mechanical Engineering, University of California, Berkeley, CA 94720, U.S.A.

(*Received* 8 *August* 1974 *and in revised form* 4 *February* 1975)

Abstract—A simple closed-form expression for the infrared emittance and the solar absorptance of honeycomb solar collectors has been obtained in terms of the passage transmittance function. The predicted results agree well with the existing data of infrared emittance for thin-walled square-cell honeycomb collectors in vacuum. A new concept of double-honeycomb structure is also introduced and analyzed. This concept provides considerable flexibility in various designs of honeycomb collectors.

NOMENCLATURE

a, constant defined in equation (5);
b, constant defined in equation (20);
e, blackbody emissive power;
L, length of the honeycomb, Figs. 1 and 2;
q, radiant energy flux;
q^*, dimensionless radiant energy flux, equation (16);
Q, incoming energy flux;
t, wall thickness;
T^1, base surface temperature;
T^2, surrounding or top surface temperature;
x, axial coordinate, Figs. 1 and 2;
y, axial coordinate, Fig. 2.

Greek symbols

α, absorptivity;
β, constant defined in equation (22);
γ, constant defined in equation (7);
ε, emissivity;
η, collector efficiency;
θ, dimensionless distance, Fig. 2;
ξ, dimensionless distance, Figs. 1 and 2;
σ, Stefan–Boltzmann constant;
τ, passage transmittance function;
Φ, dimensionless emissive power, equations (3) and (16);
ω, wall material per unit area of the honeycomb structure, Fig. 3.

Subscripts

b, blackbody;
e, effective;
i, infrared;
s, solar;
w, wall;
λ, spectral;
1, base surface;
z, top surface.

Superscripts

I, bottom honeycomb;
II, top honeycomb.

INTRODUCTION

LARGE scale utilization of solar energy, particularly in domestic heating and cooling, requires the development of an efficient, durable and low cost solar absorber. Among various designs, the honeycomb solar collector has been suggested and shown to be a very promising device for such applications [1–3]. For design and performance evaluation, the radiation characteristics of a honeycomb collector must be analyzed. In this work, a simple closed-form expression for the i.r. emittance and the solar absorptance of honeycomb collectors has been established on the basis of the passage transmittance function introduced by Edwards and Tobins [4]. Furthermore, a new concept of double-honeycomb structure is introduced for potential improvement in honeycomb solar collector design and performance. An analysis of its radiation characteristics has also been carried out.

SIMPLE HONEYCOMB SOLAR COLLECTORS

A typical portion of a honeycomb absorber is shown schematically in Fig. 1. The choice of a square-cell

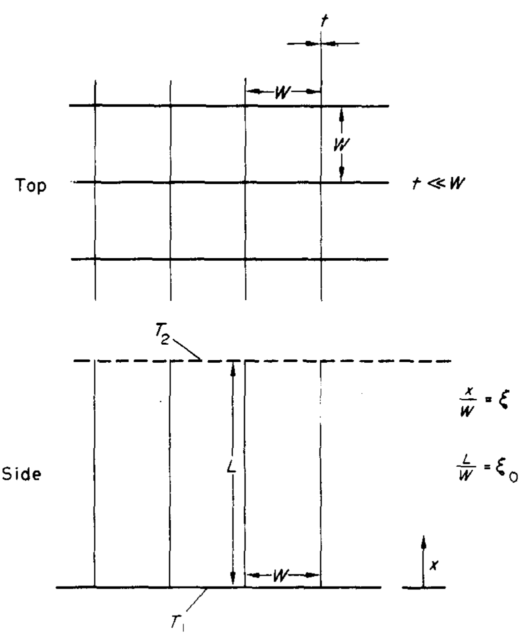

FIG. 1. The single square-honeycomb solar absorber.

honeycomb system shown in Fig. 1 is only for the purpose of illustration. The analysis developed in this work is general and applicable to honeycomb structures with any cross-sectional geometry. Due to the geometric and thermal symmetry of the honeycomb structure, the heat-transfer problem is localized and reduced to that of radiant heat transfer through each individual passage with adiabatic walls. The medium inside the passages is assumed to be non-conducting, non-absorbing and non-scattering. For convenience of discussion and without loss of generality, the surrounding atmosphere is replaced by an effective black surface at the top of the structure radiating at the ambient temperature T_2. The side wall surface is assumed to be specularly reflecting but diffusely emitting. The base surface is first considered to be black and radiating at the base temperature T_1, and the results obtained will then be generalized to include the case of non-black base surface.

The net radiant energy flux at wavelength λ in the positive x direction at a distance x from the base surface can be formulated as [4]

$$\begin{aligned} q_\lambda(x) = {} & \tau_\lambda(x)[e_{\lambda b1}-e_{\lambda b2}]+\tau_\lambda(L-x)[e_{\lambda b}(L)-e_{\lambda b2}] \\ & -\tau_\lambda(x)[e_{\lambda b}(0)-e_{\lambda b2}] \\ & -\int_0^x \tau_\lambda(x-x')\left\{\frac{\mathrm{d}}{\mathrm{d}x'}[e_{\lambda b}(x')-e_{\lambda b2}]\right\}\mathrm{d}x' \\ & -\int_x^L \tau_\lambda(x'-x)\left\{\frac{\mathrm{d}}{\mathrm{d}x'}[e_{\lambda b}(x')-e_{\lambda b2}]\right\}\mathrm{d}x' \end{aligned} \quad (1)$$

where $e_{\lambda b}$ is the blackbody emissive power and $\tau_\lambda(x)$ is the passage transmittance from the base surface to the cross-sectional plane at x including the effect of polarization and phase change in reflection but no side wall emission. Numerical values of $\tau(x)$ for various square cross-sectional passages and infinite parallel plate passages were tabulated by Edwards and Tobins [4]. Similar computation can be made for other cross-sectional geometries.

Assuming that the honeycomb wall is so thin that conduction along the wall can be neglected, the energy equation for an infinitesimal length of the wall is simply

$$\frac{\mathrm{d}q_\lambda}{\mathrm{d}x} = 0. \quad (2)$$

Introducing the non-dimensional variables

$$\xi = \frac{x}{W} \qquad \Phi(\xi) = \frac{e_{\lambda b}(\xi)-e_{\lambda b2}}{e_{\lambda b1}-e_{\lambda b2}} \quad (3)$$

equations (1) and (2) can be combined to give the effective emittance of the honeycomb collector as

$$\begin{aligned} \varepsilon_\lambda(\xi_0) = {} & \frac{q_\lambda}{e_{\lambda b1}-e_{\lambda b2}} = \tau_\lambda(\xi)+\tau_\lambda(\xi_0-\xi)\Phi_\lambda(\xi_0) \\ & -\tau_\lambda(\xi)\Phi_\lambda(0)-\int_0^\xi \tau_\lambda(\xi-\xi')\frac{\mathrm{d}\Phi_\lambda(\xi')}{\mathrm{d}\xi'}\mathrm{d}\xi' \\ & -\int_\xi^{\xi_0} \tau_\lambda(\xi'-\xi)\frac{\mathrm{d}\Phi_\lambda(\xi')}{\mathrm{d}\xi'}\mathrm{d}\xi' \end{aligned} \quad (4)$$

where

$$\xi_0 = \frac{L}{W}.$$

An approximate closed-form expression for $\varepsilon_\lambda(\xi_0)$ can be obtained using the kernel substitution technique, which substitutes $\tau_\lambda(\xi)$ by an exponential function, i.e.

$$\tau_\lambda(\xi) = \exp(-a_\lambda\xi) \quad (5)$$

where a_λ is a constant depending on the surface reflectance. The numerical solution of $\tau_\lambda(\xi)$ [4] indicates that this is a valid approximation, and accordingly a_λ can be determined by simply matching with the solution. This same approximation has been employed with great success in the calculation of lateral conduction and radiation along parallel plates [5].

Differentiating twice equations (1) and (2) gives

$$\frac{\mathrm{d}^2\Phi_\lambda(\xi)}{\mathrm{d}^2\xi} = 0. \quad (6)$$

Equation (6) can be integrated to yield

$$\Phi_\lambda(\xi) = \gamma_1\xi+\gamma_2. \quad (7)$$

Substituting equations (5) and (7) into equation (4), carrying out the integration, there result:

$$\gamma_1 = \frac{-a_\lambda}{2+a_\lambda\xi_0} \qquad \gamma_2 = \frac{1+a_\lambda\xi_0}{2+a_\lambda\xi_0} \quad (8)$$

and

$$\varepsilon_\lambda(\xi_0) = \frac{1}{1-\ln\sqrt{[\tau_\lambda(\xi_0)]}}. \quad (9)$$

For collector efficiency calculation, it is more convenient to use the average emissivity over the infrared range $\varepsilon_i(\xi_0)$. For most materials the absorptive and refractive indices vary slowly in the infrared region and can be represented by appropriate constants defined for the predominant energy-containing wavelength λ_i. In terms of infrared gray quantities, it then follows:

$$\varepsilon_i(\xi_0) = \frac{1}{1-\ln\sqrt{[\tau_{\lambda_i}(\xi_0)]}}. \quad (10)$$

It is interesting to note that this problem bears a remarkable similarity to a gaseous radiation problem. Consider an absorbing but non-emitting gas inside a vertical column with the same geometrical structure as that of a honeycomb. If $\tau_\lambda(x)$ is interpreted as the transmission of radiation through the absorbing gas from the base surface to a cross-sectional area at vertical distance x, the heat flux through the passage is given by equation (1), and equation (10) is the closed-form expression for the non-dimensional heat flux. The combined effect of absorption and reflection by the honeycomb wall is identical to the effect of putting a layer of absorbing but non-emitting gas above the absorbing base surface.

Using the gaseous radiation analogy, the generalization of equation (10) to collectors with non-black absorbing base surface is straightforward. Using exactly the same arguments as in gaseous radiation [6], it can be shown that the effective i.r. emissivity is given by

$$\varepsilon_{ie}(\xi_0) = \frac{1}{\dfrac{1}{\varepsilon_b}-\ln\sqrt{[\tau_{\lambda_i}(\xi_0)]}} \quad (11)$$

where ε_b is the i.r. emissivity of the base surface.

Arguments leading to equations (10) and (11) can be carried out analogously for solar energy absorption. Applying Kirchhoff's law, the effective solar absorptance of the honeycomb collector is

$$\alpha_{se}(\xi_0) = \frac{1}{\dfrac{1}{\alpha_s} - \ln\sqrt{[\tau_{\lambda,s}(\xi_0)]}} \qquad (12)$$

where α_s is the solar absorptivity of the base surface.

With equations (10) and (11), the efficiency of a simple honeycomb solar collector operating with the incoming solar flux Q_s, the absorber base temperature T_1 and the ambient atmospheric temperature T_2, is given by

$$\eta(\xi_0) = \alpha_{se} - \frac{\varepsilon_{ie}(\xi_0)[\sigma T_1^4 - \sigma T_2^4]}{Q_s}. \qquad (13)$$

DOUBLE HONEYCOMB SOLAR ABSORBERS

The basic geometry and nomenclature used in the analysis of radiative heat transfer in a double honeycomb solar absorber is shown in Fig. 2. Again, there is

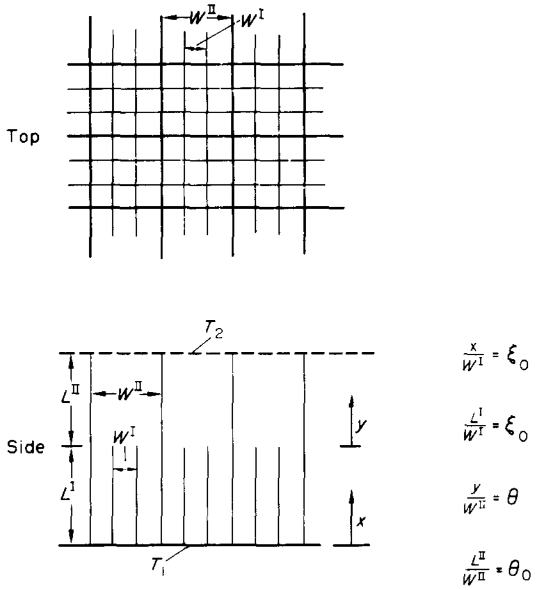

FIG. 2. The double square-honeycomb solar absorber.

no assumption on cross-sectional geometry in this analysis and the choice of a square-cell structure in Fig. 2 is abritrary. Using the same assumptions as those in the analysis of the simple honeycomb, the net radiant energy flux in the positive x direction can be formulated as

$$\begin{aligned} q_\lambda(x) &= e_{\lambda b1}\tau^I_\lambda(x) - e_{\lambda b2}\tau^I_\lambda(L^I - x)\tau^{II}_\lambda(L^{II}) \\ &+ \int_0^x e_{\lambda b}(x')\frac{d\tau^I_\lambda(x-x')}{d(x-x')}d(x-x') \\ &+ \int_x^{L^I} e_{\lambda b}(x')\frac{d\tau^I_\lambda(x'-x)}{d(x'-x)}d(x'-x) \\ &+ \tau^I_\lambda(L^I - x)\int_0^{L^{II}} e_{\lambda b}(y')\frac{d\tau^{II}_\lambda(y')}{dy'}dy'. \end{aligned} \qquad (14)$$

The net radiant energy flux in the positive y direction is

$$\begin{aligned} q_\lambda(y) &= e_{\lambda b1}\tau^I_\lambda(L^I)\tau^{II}_\lambda(y) - e_{\lambda b2}\tau^{II}_\lambda(L^{II} - y) \\ &+ \int_0^{L^I} \tau^{II}_\lambda(y)e_{\lambda b}(x')\frac{d\tau^I_\lambda(L^I - x')}{d(L^I - x')}d(L^I - x') \\ &+ \int_0^y e_{\lambda b}(y')\frac{d\tau^{II}_\lambda(y-y')}{d(y-y')}d(y-y') \\ &+ \int_y^{L^{II}} e_{\lambda b}(y')\frac{d\tau^{II}_\lambda(y'-y)}{d(y'-y)}d(y'-y) \end{aligned} \qquad (15)$$

where $\tau^I_\lambda(x)$ and $\tau^{II}_\lambda(y)$ are transmittance functions of the bottom and top honeycombs respectively, and L^I, W^I, L^{II}, W^{II} are geometric dimensions defined in Fig. 2. Introducing non-dimensional variables

$$\begin{aligned} &\xi = \frac{x}{W^I} \quad \theta = \frac{y}{W^{II}} \quad \Phi^I_\lambda(x) = \frac{e_{\lambda b}(x) - e_{\lambda b2}}{e_{\lambda b1} - e_{\lambda b2}} \\ &q^*_\lambda(x) = \frac{q_\lambda(x)}{e_{\lambda b1} - e_{\lambda b2}} \quad q^*_\lambda(y) = \frac{q_\lambda(y)}{e_{\lambda b1} - e_{\lambda b2}} \\ &\Phi^{II}_\lambda(y) = \frac{e_{\lambda b}(y) - e_{\lambda b2}}{e_{\lambda b1} - e_{\lambda b2}} \end{aligned} \qquad (16)$$

and integrating by parts, equations (14) and (15) can be rewritten in a more convenient form.

$$\begin{aligned} q^*_\lambda(\xi) &= \tau^I_\lambda(\xi)[1 - \Phi^I_\lambda(0)] + \tau^I_\lambda(\xi_0 - \xi)[\Phi^I_\lambda(\xi_0) - \Phi^{II}_\lambda(0)] \\ &+ \tau^I_\lambda(\xi_0 - \xi)\Phi^{II}_\lambda(\theta_0)\tau^{II}_\lambda(\theta_0) - \int_0^\xi \tau^I_\lambda(\xi - \xi')\frac{d\Phi^I}{d\xi'}d\xi' \\ &- \int_\xi^{\xi_0} \tau^I_\lambda(\xi' - \xi)\frac{d\Phi^I}{d\xi'}d\xi' - \tau^I_\lambda(\xi_0 - \xi) \\ &\times \int_0^{\theta_0} \tau^{II}_\lambda(\theta)\frac{d\Phi^{II}}{d\theta}d\theta \end{aligned} \qquad (17)$$

where

$$\xi_0 = \frac{L^I}{W^I} \qquad \theta_0 = \frac{L^{II}}{W^{II}}$$

and

$$\begin{aligned} q^*_\lambda(\theta) &= \tau^I_\lambda(\xi_0)\tau^{II}_\lambda(\theta) + \tau^{II}_\lambda(\theta)[\Phi^I_\lambda(\xi_0) - \Phi^{II}_\lambda(0)] \\ &- \Phi^I_\lambda(0)\tau^I_\lambda(\xi_1)\tau^{II}_\lambda(0) + \Phi^{II}_\lambda(\theta_0)\tau^{II}_\lambda(\theta_0 - \theta) \\ &- \int_0^{\xi_0} \tau^{II}_\lambda(\theta)\tau^I_\lambda(\xi_0 - \xi')\frac{d\Phi^I}{d\xi'}d\xi' - \int_0^\theta \frac{d\Phi^{II}_\lambda}{d\theta'} \\ &\times \tau^{II}_\lambda(\theta - \theta')d\theta' - \int_\theta^{\theta_0} \tau^{II}_\lambda(\theta' - \theta)\frac{d\Phi^{II}_\lambda}{d\theta'}d\theta'. \end{aligned} \qquad (18)$$

The assumption of adiabatic and non-conducting wall again gives the following energy equation,

$$\frac{dq^*_\lambda(\theta)}{d\theta} = \frac{dq^*_\lambda(\xi)}{d\xi} = 0. \qquad (19)$$

The apparent emissivity of the double honeycomb solar absorber is

$$\varepsilon_\lambda(\xi_0, \theta_0) = q^*_\lambda(\xi) = q^*_\lambda(\theta).$$

Equations (17)–(19) can again be solved by the kernel substitution technique. The transmittance functions $\tau^I_\lambda(\xi)$ and $\tau^{II}_\lambda(\theta)$ are approximated by exponential functions as follows:

$$\tau^I_\lambda(\xi) = \exp(-b_{I\lambda}\xi) \qquad \tau^{II}_\lambda(\theta) = \exp(-b_{II\lambda}\theta) \qquad (20)$$

where $b_{I\lambda}$ and $b_{II\lambda}$ are constants depending on the surface properties. Differentiating twice equations (17)–(19) gives

$$\frac{d^2\Phi^{I}_{\lambda}}{d\xi^2} = 0 \qquad \frac{d^2\Phi^{II}_{\lambda}}{d\theta^2} = 0 \tag{21}$$

which yield

$$\Phi^{I}_{\lambda}(\xi) = \beta_1 \xi + \beta_2 \qquad \Phi^{II}_{\lambda}(\theta) = \beta_3 \theta + \beta_4. \tag{22}$$

By substituting equations (20) and (22) into equations (17) and (18), the solutions are

$$\beta_1 = \frac{-b_{I\lambda}}{2+b_{I\lambda}\xi_0+b_{II\lambda}\theta_0} \qquad \beta_2 = \frac{1+b_{I\lambda}\xi_0+b_{II\lambda}\theta_0}{2+b_{I\lambda}\xi_0+b_{II\lambda}\theta_0} \tag{23}$$

$$\beta_3 = \frac{-b_{II\lambda}}{2+b_{I\lambda}\xi_0+b_{II\lambda}\theta_0} \qquad \beta_4 = \frac{1+b_{II\lambda}\theta_0}{2+b_{I\lambda}\xi_0+b_{II\lambda}\theta_0}$$

and

$$\varepsilon_{\lambda}(\xi_0, \theta_0) = \frac{1}{1-\ln\sqrt{[\tau^{I}_{\lambda}(\xi_0)\tau^{II}_{\lambda}(\theta_0)]}}. \tag{24}$$

If the two sections of the double honeycomb are made of the same material, $b_{I\lambda}$ and $b_{II\lambda}$ are identical. The apparent emissivity is given by

$$\varepsilon_{\lambda}(\xi_0, \theta_0) = \frac{1}{1-\ln\sqrt{[\tau_{\lambda}(\xi_0+\theta_0)]}}. \tag{25}$$

The double honeycomb problem also draws an analogy to a gaseous radiation problem. The effect of reflection and absorption by the walls of the double honeycomb is identical to the effect of putting two layers of absorbing but non-emitting gases with transmittance functions τ^{I}_{λ} and τ^{II}_{λ}. Using the same arguments as those for the simple honeycomb, the i.r. emittance and the solar absorptance are given by

$$\varepsilon_{ie}(\xi_0, \theta_0) = \frac{1}{\frac{1}{\varepsilon_b} - \ln\sqrt{[\tau_{\lambda_i}(\xi_0+\theta_0)]}} \tag{26}$$

$$\alpha_{se}(\xi_0, \theta_0) = \frac{1}{\frac{1}{\alpha_s} - \ln\sqrt{[\tau_{\lambda_s}(\xi_0+\theta_0)]}}. \tag{27}$$

RESULTS AND DISCUSSION

Experimental data of radiant heat transmission through a honeycomb solar collector are relatively scarce in the literature. Moreover, most data are not directly applicable for comparison here because they were measured under the condition in which convection and conduction are the dominant mode of heat transfer. The recent experimental investigation by Cunnington and Streed [3], however, does provide the emittance data of thin-walled square-cell honeycombs in vacuum. A summary of their measurements and the corresponding calculated values from equation (11) are given in Table 1. The agreements are excellent except for the case of aluminum honeycomb. The discrepancy for the aluminum case is not too surprising because aluminum has a large thermal conductivity and the assumption of negligible conductive heat transfer may cause errors.

It is interesting to note that equation (11) gives excellent agreement with experimental data even for the aluminum honeycomb, where the assumption of negligible conduction heat transfer along the wall is no longer applicable. This result is not too surprising because aluminum, like all materials with large thermal conductivity, has large reflectivity. For such material, the net radiant heat flux leaving the honeycomb given by equation (1) is relatively insensitive to the error in the temperature profile used. Consequently, the temperature profile predicted by the low conductivity assumption introduces only slight errors in the heat flux calculation.

The net infrared radiant heat-transfer rate for a honeycomb with perfectly conducting wall is given by [4]

$$q_i = 0{\cdot}5[1+\tau_{\lambda i}(\rho_0)](\sigma T_1^4 - \sigma T_2^4). \tag{28}$$

The effective emissivity calculated from the above expression agrees almost exactly with the result of equation (11) for the aluminum honeycomb and differs only slightly for the mylar and paper honeycombs. This

Table 1. Measured and predicted infrared emittance of honeycomb collectors

Wall material	ρ_w*	L/W	$\tau(L/W)$†	ε_b	Infrared emittance of honeycomb: Measured [3]	Predicted
Aluminum	0·95	5·33	0·7979	0·91	0·76	0·83
				0·94	0·78	0·85
				0·95	0·79	0·86
Mylar	0·16	1·67	0·1877	0·91	0·50	0·52
				0·94	0·56	0·53
				0·95	0·59	0·53
				0·11	0·09	0·10
				0·14	0·12	0·13
Paper	0·10	5·33	0·0376	0·91	0·30	0·37
				0·94	0·32	0·37
				0·95	0·33	0·37

*Values measured at room temperature.
†The value of $\tau(L/W)$ is obtained by linear extrapolation from results in [5].

result demonstrates explicitly that equation (11) is an excellent approximation of the infrared emittance of a honeycomb solar absorber.

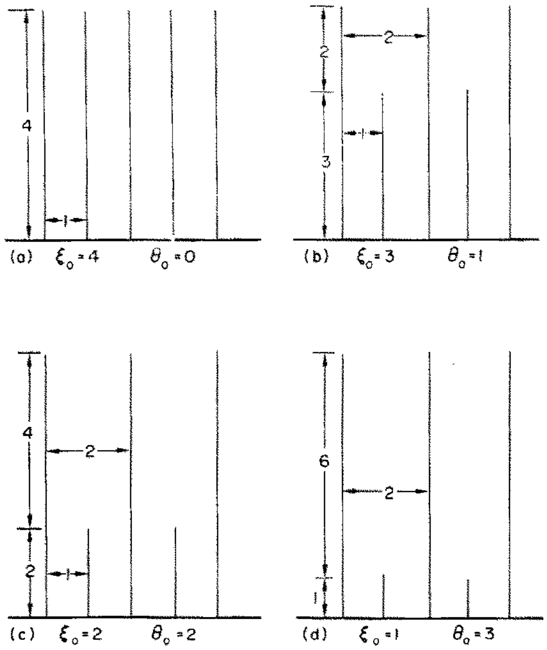

FIG. 3. Various designs of the double square-honeycomb with identical radiation characteristics.

No experimental work has ever been done on a double honeycomb solar collector. But theoretically, it can be seen that this idea provides great flexibility in the actual design of solar collectors. The main conclusion from equations (26) and (27) is that any double honeycomb solar collector with the same sum of aspect ratio $(\xi_0+\theta_0)$ has the same radiative thermal efficiency. Figure 3 shows the side view of four different designs of square-cell double honeycomb with the same radiative characteristics. It is interesting to note that each design requires the same amount of wall material per unit base surface area (designated as ω) and therefore has about the same cost. In fact, it can be easily shown that any honeycomb structure with the same value of ω has the same radiative characteristic. The designer thus has the freedom to choose a most efficient design with desirable values of ω and η on the basis of conduction and convection considerations, collector durability, and other solar collector design criteria.

REFERENCES

1. K. G. T. Hollands, Honeycomb devices in flat-plate solar collectors, *Solar Energy* **9**, 159–164 (1965).
2. H. Buckberg, O. H. Lalude and D. K. Edwards, Performance characteristics of rectangular honeycomb solar-thermal converters, *Solar Energy* **13**, 193–221 (1971).
3. G. R. Cunnington and E. R. Streed, Experimental performance of a honeycomb covered flat plate solar collector, *Proceedings of 1973 International Solar Energy Conference*, Cleveland, Ohio (October, 1973).
4. D. K. Edwards and R. D. Tobins, Effect of polarization on radiant heat transfer through long passages, *J. Heat Transfer* **89C**, 132–138 (1967).
5. C. L. Tien, P. S. Jagannathan and B. F. Armaly, Analysis of lateral conduction and radiation along two parallel long plates, *AIAA Jl* **7**, 1806–1808 (1969).
6. R. Siegel and J. R. Howell, *Thermal Radiation Heat Transfer*. McGraw-Hill, New York (1972).

CARACTERISTIQUES DE RAYONNEMENT DES COLLECTEURS SOLAIRES A NID D'ABEILLES

Résumé—On a obtenu une expression simple de l'émission infrarouge et de l'absorption solaire des collecteurs solaires à nid d'abeilles à l'aide de la fonction de transfert. Les résultats des prévisions sont en bon accord avec les données existentes sur l'émission infrarouge pour des collecteurs à nid d'abeilles à cellules carrées et parois minces dans le vide. On a également introduit un nouveau concept de structure à double nid d'abeilles. Ce concept permet une grande souplesse dans les divers schémas de collecteurs à nid d'abeilles.

STRAHLUNGSEIGENSCHAFTEN VON SONNENKOLLEKTOREN IN WABENBAUWEISE

Zusammenfassung—Ein einfacher Ausdruck in geschlossener Form für die Infrarot-Emission und die Solar-Absorption für Sonnenkollektoren in Wabenbauweise wurde abgeleitet in Form der "Durchgangs-Durchlässigkeits-Funktion". Die Berechnungsergebnisse stimmen gut mit den vorhandenen Werten für Infrarot-Emission von dünnwandigen, quadratzelligen Wabenkollektoren im Vakuum überein. Es wird ein neuer Vorschlag für eine Doppelwabenstruktur vorgestellt und analysiert. Dieser Entwurf ermöglicht beträchtliche Flexibilität bei unterschiedlichen Ausführungen von Wabenkollektoren.

РАДИАЦИОННЫЕ ХАРАКТЕРИСТИКИ СОТОВЫХ СОЛНЕЧНЫХ БАТАРЕЙ

Аннотация — В виде функции прозрачности канала получено простое выражение замкнутого типа для коэффициентов испускания инфракрасного излучения и поглощения солнечных лучей сотовыми солнечными батареями. Расчетные данные хорошо согласуются с имеющимися по коэффициенту испускания инфракрасного излучения солнечных батарей с тонкостенными квадратными ячейками, работающих в вакууме. Вводится и анализируется новая конструкция двойной ячеистой структуры. В результате использования этой конструкции можно добиться значительной гибкости в работе различных конструкций сотовых батарей.